

Document downloaded from:

<http://hdl.handle.net/10251/61108>

This paper must be cited as:

Bonancía Roca, P.; Vayá Pérez, I.; Markovitsi, D.; Gustavsson, T.; Jiménez Molero, MC.; Miranda Alonso, MÁ. (2013). Stereodifferentiation in the intramolecular singlet excited state quenching of hydroxybiphenyl-tryptophan dyads. *Organic and Biomolecular Chemistry*. 11(12):1958-1963. doi:10.1039/c3ob27278h.



The final publication is available at

<http://dx.doi.org/10.1039/c3ob27278h>

Copyright Royal Society of Chemistry

Additional Information

# Stereodifferentiation in the Intramolecular Singlet Excited State Quenching of Hydroxybiphenyl/Tryptophan Dyads

Paula Bonancía,<sup>a</sup> Ignacio Vayá,<sup>a</sup> Dimitra Markovitsi,<sup>b</sup> Thomas Gustavsson,<sup>b</sup> M. Consuelo Jiménez<sup>\*a</sup> and Miguel A. Miranda<sup>\*a</sup>

The photochemical processes occurring in diastereomeric dyads (*S,S*)-**1** and (*S,R*)-**1**, prepared by conjugation of (*S*)-2-(2-hydroxy-1,1'-biphenyl-4-yl)propanoic acid ((*S*)-**BPOH**) with (*S*)- and (*R*)-**Trp**, have been investigated. In acetonitrile, the fluorescence spectra of (*S,S*)-**1** and (*S,R*)-**1** were coincident in shape and position with that of (*S*)-**BPOH**, although they revealed a markedly stereoselective quenching. Since singlet energy transfer from **BPOH** to **Trp** is forbidden (5 kcal mol<sup>-1</sup> uphill), the quenching was attributed to thermodynamically favoured (according to Rehm-Weller) electron transfer or exciplex formation. Upon addition of 20% water, the fluorescence quantum yield of (*S*)-**BPOH** decreased, while only minor changes were observed for the dyads. This can be explained by an enhancement of the excited state acidity of (*S*)-**BPOH**, associated with bridging of the carboxy and hydroxy groups by water, in agreement with the presence of water molecules in the X-ray structure of (*S*)-**BPOH**. When the carboxy group was not available for coordination with water, as in the methyl ester (*S*)-**BPOHMe** or in the dyads, this effect was prevented; accordingly, the fluorescence quantum yields did not depend on the presence or absence of water. The fluorescence lifetimes in dry acetonitrile were 1.67, 0.95 and 0.46 ns for (*S*)-**BPOH**, (*S,S*)-**1** and (*S,R*)-**1**, respectively, indicating that the observed quenching is indeed dynamic. In line with the steady-state and time-resolved observations, molecular modelling pointed to a more favourable geometric arrangement of the two interacting chromophores in (*S,R*)-**1**. Interestingly, this dyad exhibited a folded conformation in the solid state.

## Introduction

Bichromophoric compounds incorporating two photoactive moieties are useful models to gain insight into key mechanistic aspects of light-induced processes. In this context, intramolecular energy, proton or electron transfer, as well as exciplex formation and photochemical reactivity, have received considerable attention.<sup>1</sup> These processes have been investigated in a variety of systems, including dyads containing a non-steroidal anti-inflammatory drug (NSAID) covalently linked to a biomimetic substructure (for instance, an amino acid or a nucleoside, as models for proteins or DNA).<sup>2</sup> Specifically, previous efforts have been devoted to the photophysical study of dyads containing NSAIDs and the amino acid tryptophan (**Trp**), as valuable tools to provide relevant information on drug-protein interactions within the binding sites.<sup>3</sup> In this context, steady-state and time-resolved fluorescence spectroscopy has been widely used to address a variety of biological problems,<sup>4</sup> including the excited state interactions between proteins and complexed ligands.<sup>5</sup>

The photophysical behaviour of diastereomeric dyads containing the biphenyl-like NSAID flurbiprofen ((*S*)-**FBP**, Chart

1) and **Trp** has recently been described.<sup>6</sup> Upon irradiation at 266 nm, both chromophores are excited, but only **Trp** emission ( $E_s = 96$  kcal mol<sup>-1</sup>) is detected. Moreover, stereoselective intramolecular <sup>1</sup>**Trp**\* charge transfer quenching is observed, accompanied by formation of exciplexes. Indeed, the absorption and emission properties of **Trp** are very sensitive to the local environment<sup>7</sup> and have been employed to investigate structural changes of protein functions<sup>8</sup> and to address the protein binding of endogenous and exogenous agents (such as drugs, fatty acids, metabolites).<sup>9</sup>

Attachment of a hydroxy group at the *ortho* position of a biphenyl results in a significant decrease of its singlet energy (*ca.* 10 kcal mol<sup>-1</sup>) and provides an additional deactivation pathway, namely excited state intramolecular proton transfer (ESIPT). As ESIPT is in general a reversible process,<sup>10</sup> it has found application for the design of photostabilizers, solar filters, solar energy collectors, etc.<sup>11</sup> In hydroxybiphenyls, ESIPT occurs from the acidic phenolic proton to the sp<sup>2</sup> hybridized 2'-carbon of the aromatic ring, giving rise to a reactive quinone methide. In addition, intermolecular excited state deprotonation is observed in

the presence of bulk water, to give the corresponding phenolate.<sup>12</sup>

With this background, we have now investigated the photophysical processes occurring in diastereomeric dyads (*S,S*)-**1** and (*S,R*)-**1** (Chart 1), which contain a chiral 2-hydroxybiphenyl derivative covalently linked to **Trp**.

## Results and Discussion

The required (*S*)-2-(2-hydroxy-1,1'-biphenyl-4-yl)propanoic acid ((*S*)-**BPOH**) was readily obtained by irradiation of (*S*)-**FBP** in aqueous media, through a photonucleophilic substitution.<sup>13</sup> The dyads (*S,S*)-**1** and (*S,R*)-**1** were prepared by conjugation of ((*S*)-**BPOH**) with the (*S*)- or (*R*)- methyl ester of tryptophan (**TrpMe**), using a carbodiimide as activating agent. The chemical structures are shown in Chart 1.

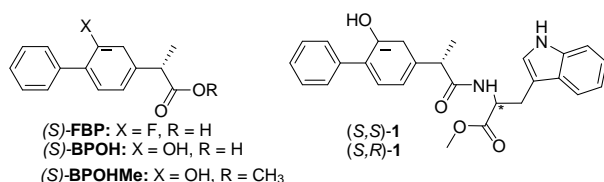


Chart 1

The UV-Vis absorption spectrum of (*S,S*)-**1** in MeCN is shown in Figure 1, together with those of (*S*)-**FBP** and (*S*)-**BPOH** for comparison. It can be observed that replacement of fluorine by hydroxyl induces a bathochromic shift of the longer wavelength band. The spectra of (*S,S*)-**1** and (*S,R*)-**1** were coincident and matched with that obtained upon addition of the absorption spectra of the isolated chromophores ((*S*)-**BPOH** and (*S*)-**TrpMe**), indicating the absence of significant interactions between the two moieties in the ground state.

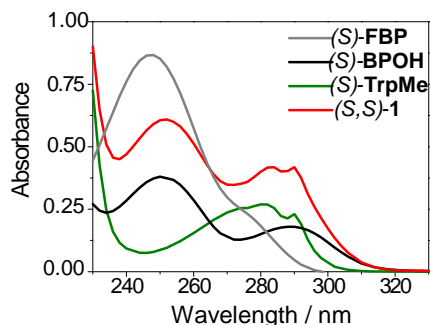


Figure 1. UV-Vis absorption spectra of (*S*)-**FBP** (grey), (*S*)-**BPOH** (black), (*S*)-**TrpMe** (green) and (*S,S*)-**1** (red) in acetonitrile at 5 × 10<sup>-5</sup> M concentration.

The fluorescence spectra of (*S,S*)-**1** and (*S,R*)-**1**, obtained after excitation at λ = 267 nm in MeCN/air, are shown in Figure 2 (solid lines) together with that of (*S*)-**BPOH**. All the emissions consisted in a structureless band centered at ca. 330 nm (Table 1). In the dyads, the incident photons are absorbed by both the hydroxybiphenyl chromophore and the **Trp** moiety (Figure 1); however, no **Trp** contribution was observed in the fluorescence spectra, which were coincident in shape and position with that of (*S*)-**BPOH**. From the intersection between the excitation (λ<sub>em</sub> = 330 nm) and emission (λ<sub>exc</sub> = 267 nm) normalised bands (Figure

S4 in ESI), a singlet energy value of ca. 91 kcal mol<sup>-1</sup> was obtained for (*S*)-**BPOH**, (*S,S*)-**1** and (*S,R*)-**1**.

In the dyads, the most remarkable observation was a dramatic quenching, which turned out to be stereoselective (see Table 1). Since SSET from (*S*)-**BPOH** to **Trp** is thermodynamically forbidden, the observed quenching was in principle attributed to electron transfer or exciplex formation.

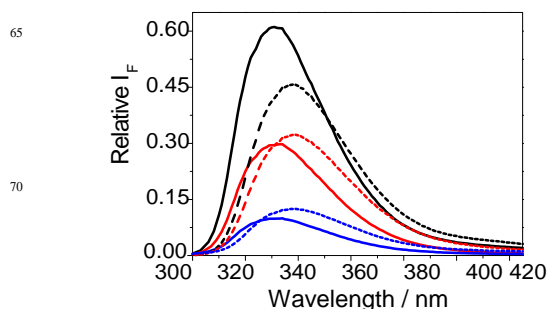


Figure 2. Fluorescence spectra of (*S*)-**BPOH** (black), (*S,S*)-**1** (red) and (*S,R*)-**1** (blue) at λ<sub>exc</sub> = 267 nm, under air. Solid lines: MeCN; dashed lines: MeCN/H<sub>2</sub>O 4:1.

The feasibility of formation of radical ion pairs or exciplexes from the singlet excited state can be estimated by application of the Rehm-Weller equations.<sup>14</sup> Taking into account the corresponding oxidation (E<sub>OX</sub>) and reduction (E<sub>RED</sub>) potentials,<sup>15</sup> the appropriate dielectric constants (ε)<sup>16</sup> and the (*S*)-**BPOH** singlet energy (E<sub>S</sub> = 91 kcal mol<sup>-1</sup>), a favourable thermodynamics was anticipated for charge transfer quenching *via* both electron transfer and exciplex formation (see Table S1 in p. S6 of ESI). These processes are more likely to occur in folded conformations, since a close contact is required between the donor and acceptor moieties. As a matter of fact, the (*S,R*)-diastereomer exhibited a folded conformation in the solid state, as shown by X-ray diffraction (Figure 3). Interestingly, quenching was more efficient in this dyad than in (*S,S*)-**1**.

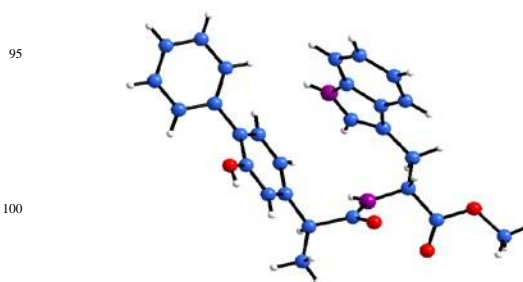


Figure 3. X-ray structure of compound (*S,R*)-**1**.

To check whether ESIPT from the acidic phenolic proton to the sp<sup>2</sup> hybridised 2'-carbon of the neighbouring aromatic ring could play a role in these systems, in competition with charge transfer quenching, a 20% of water was added (dashed lines in Figure 2). This water content should be low enough as to prevent intermolecular excited state deprotonation to bulk water, giving the corresponding phenolate.

**Table 1.** Relevant photophysical parameters for (*S*)-**BPOH**, (*S*)-**BPOHMe**, (*S,S*)-**1** and (*S,R*)-**1**.<sup>a</sup>

	MeCN				MeCN/H <sub>2</sub> O			
	( <i>S</i> )- <b>BPOH</b>	( <i>S</i> )- <b>BPOHMe</b>	( <i>S,S</i> )- <b>1</b>	( <i>S,R</i> )- <b>1</b>	( <i>S</i> )- <b>BPOH</b>	( <i>S</i> )- <b>BPOHMe</b>	( <i>S,S</i> )- <b>1</b>	( <i>S,R</i> )- <b>1</b>
$\lambda_{em}$ (nm)	331	334	330	332	338	340	339	339
$\phi_F^b$	0.241	0.290	0.116	0.042	0.200	0.280	0.139	0.060
$\tau_F$ (ns) <sup>c</sup>	1.67	2.10	0.95	0.46	1.27	1.80	1.07	0.57
$k_F \times 10^8$ (s <sup>-1</sup> ) <sup>d</sup>	1.43	1.38	1.22	0.91	1.57	1.55	1.29	1.05
$k_Q \times 10^8$ (s <sup>-1</sup> ) <sup>e</sup>	-	-	4.5	15.8	-	-	1.5	9.7
$\phi_{Q(ov)}^f$	-	-	0.52	0.83	-	-	0.31	0.70
$\phi_{Q(dyn)}^g$	-	-	0.43	0.68	-	-	0.16	0.55

<sup>a</sup>The absorbance of the samples was 0.2 at the excitation wavelength. <sup>b</sup> $\lambda_{exc} = 267$  nm, air, (*S*)-Trp in water as standard ( $\phi_{std} = 0.13$ ); <sup>c</sup> $\lambda_{em} = 330$  nm; <sup>d</sup> $k_F = \phi_F/\tau_F$ ; <sup>e</sup> $k_Q = (1/\tau_{F(dyad)} - 1/\tau_{F(BPOH)})$ ; <sup>f</sup> $\phi_{Q(ov)} = [1 - (\phi_{F(dyad)}/\phi_{F(BPOH)})]$ ; <sup>g</sup> $\phi_{Q(dyn)} = \phi_{F(dyad)}k_{Q(dyad)}/k_{F(dyad)}$ .

In this solvent mixture, the emission maxima were red-shifted, due to the enhanced medium polarity. Remarkably, the fluorescence quantum yield of (*S*)-**BPOH** was clearly lower than in dry MeCN, while only minor changes were observed for the dyads (Table 1). A similar trend has been reported for the model compound 2-hydroxybiphenyl under related conditions (acetonitrile containing 10 M water), although fluorescence quenching occurs to a lesser extent.<sup>12</sup> The interesting effect observed with (*S*)-**BPOH** in the presence of water can be explained by an enhancement of the excited phenol acidity, associated with bridging of the carboxy and hydroxy groups by water. As a matter of fact, this situation is clearly observed in the X-ray structure of (*S*)-**BPOH**, which actually crystallizes with a water molecule (Figure 4A). This effect should be, in principle, avoided by preventing water-mediated bridging between carboxy and hydroxy groups.

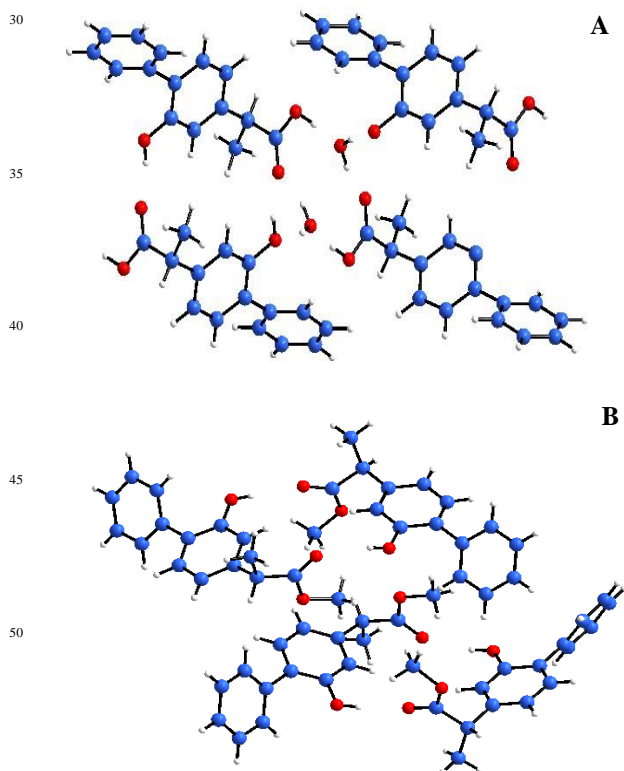


**Figure 4.** Fragment of the unit cell for A: (*S*)-**BPOH** and B: (*S*)-**BPOHMe**.

With this purpose, we synthesized the methyl ester (*S*)-**BPOHMe**. As anticipated, the fluorescence quantum yields of this model remained practically constant in the presence and absence of water (Table 1). Accordingly, water molecules were absent in the X-ray structure of (*S*)-**BPOHMe** (Figure 4B). In the case of the dyads, the acidity of the phenolic group is not enhanced as in (*S*)-**BPOH**, because the carboxy group is employed in the construction of the amide linker and is not available for coordination with water. In fact, no water molecules were found in the crystalline samples.

The fluorescence lifetimes were determined by the time-correlated single photon counting (TCSPC) technique (Figure 5). In dry acetonitrile,  $\tau_F$  ((*S*)-**BPOH**) was found to be 1.67 ns, while  $\tau_F$  values of 0.95 and 0.46 ns were measured for (*S,S*)-**1** and (*S,R*)-**1**, respectively (Table 1). This indicates that most of the overall quenching observed in the steady-state experiments is indeed dynamic, as expected for a charge transfer process (compare the two sets of values in Table 1). In the presence of water, a decrease of the (*S*)-**BPOH** fluorescence lifetime was noticed, confirming again a dynamic quenching, in agreement with an enhanced participation of the ESIPT route. As discussed above, this deactivation channel does not operate in the dyads, where the carboxylate function is involved in formation of the amide bond.

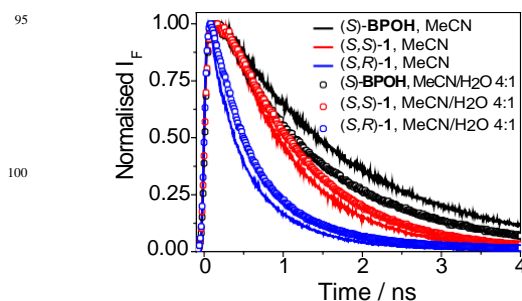


**Figure 5.** Kinetic decay traces ( $\lambda_{exc} = 267$  nm,  $\lambda_{em} = 330$  nm,  $A_{267} = 0.2$ ) for (*S*)-**BPOH** (black), (*S,S*)-**1** (red) and (*S,R*)-**1** (blue) under air, in MeCN (solid line) and MeCN/H<sub>2</sub>O 4:1 (open circles).

The quenching rate constants ( $k_Q$ ), determined from the fluorescence lifetimes  $\tau_F$ , were in the range  $10^8$ - $10^9$  s<sup>-1</sup>; as regards the radiative rate constants  $k_F$ , they were obtained from the values of  $\tau_F$  and  $\phi_F$  and found to be in the order of  $10^8$  s<sup>-1</sup> (Table 1). In order to get insight into the geometrical arrangement of the two chromophores in the dyads, which is closely related with the fluorescence quenching by charge transfer, simple molecular modelling (PM3) was performed with both (*S,S*)-**1** and (*S,R*)-**1** (see Figure 6).

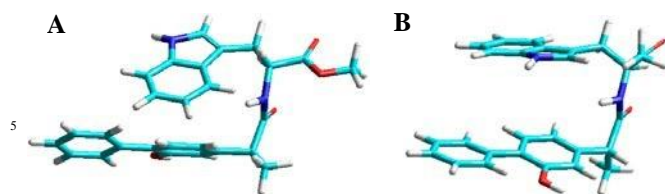


**Figure 6.** Geometry optimised (HyperChem Release 8.0.3 for Windows Molecular Model System, PM3) structure for (*S,S*)-**1** (A) and (*S,R*)-**1** (B).

Thus, (*S,R*)-**1** (Figure 6B) presented a more favourable geometric arrangement of the two interacting chromophores compared to the (*S,S*)-dyad (Figure 6A), whose geometry is more distorted, with the indole chromophore nearly orthogonal to the biphenyl moiety, which makes more difficult the interchromophoric interaction. This is in good agreement with the steady-state and time-resolved observations of lower  $\phi_F$  and shorter  $\tau_F$  values for the (*S,R*)-diastereomer.

## Conclusions

The (*S*)-**BPOH** chromophore dominates the fluorescence spectra of diastereomeric dyads (*S,S*)-**1** and (*S,R*)-**1** in acetonitrile, which reveal a substantial intramolecular charge transfer quenching with remarkable stereodifferentiation. In the presence of water (20%), the fluorescence quantum yield of (*S*)-**BPOH** decreases; by contrast, only minor changes are observed for (*S,S*)-**1** and (*S,R*)-**1**. Being (*S*)-**BPOH** a phenol, this is attributed to a water-assisted enhancement of its excited state acidity, a hypothesis that is supported by the presence of water molecules linking the carboxy and hydroxy groups in the crystalline structure. This effect is prevented in the dyads, whose fluorescence quantum yields do not depend on the presence or absence of water. The dynamic nature of the observed quenching is evidenced by a configuration-dependent shortening of the fluorescence lifetimes in (*S,S*)-**1** and (*S,R*)-**1** compared to (*S*)-**BPOH**. In agreement with the steady-state and time-resolved experimental results, molecular modelling points to a more favourable geometric arrangement of the two interacting chromophores in (*S,R*)-**1** than in (*S,S*)-**1**; this is validated by the X-ray analysis, indicating that the former dyad exhibits a folded conformation in the solid state.

## Materials and Methods

Commercial (*S*)-**FBP**, (*S*)- and (*R*)-**TrpMe**, 1-(3-dimethylaminopropyl)-*N*-ethylcarbodiimide hydrochloride (EDC) and 1-hydroxybenzotriazole (BtOH) were purchased from Sigma-Aldrich. Their purity was checked by  $^1\text{H}$  NMR and HPLC analysis. Spectrophotometric HPLC or reagent grade solvents were obtained from Scharlab and used without further purification. Solutions of phosphate-buffered saline (PBS) (0.01 M, pH 7.4) were prepared by dissolving phosphate-buffered saline tablets (from Sigma) in Milli-Q water. The  $^1\text{H}$ -NMR and  $^{13}\text{C}$ -NMR spectra were recorded in  $\text{CDCl}_3$  at 300 and 75 MHz, respectively, using a Varian Gemini instrument; chemical shifts are reported in ppm. Exact mass values were obtained in Servicio de Espectroscopía de Masas de la Universidad de Valencia. The X-ray structures were determined at Unidade de Raios X, at the Universidade de Santiago de Compostela. Crystallographic data

(excluding structure factors) for the structures of (*S*)-**BPOH**, (*S*)-**BPOHMe** and (*S,R*)-**1** have been deposited at the Cambridge Crystallographic Data Centre as supplementary publication numbers CCDC 662956, CCDC 910283 and CCDC 910284, respectively. Isolation and purification were done by conventional column chromatography on silica gel Merck 60 (0.063-0.200 mm), or by preparative layer chromatography on silica gel Merck 60 PF254, using hexane/ethyl acetate as eluent.

## Synthesis of the new compounds

**(S)-BPOH.** A solution of (*S*)-**FBP** (100 mL, 5 mM) in PBS was irradiated for 9 h through quartz, inside a Luzchem multilamp photoreactor, with the light from ten 8W lamps emitting mainly at 254 nm. The photomixture was acidified with HCl, extracted with methylene chloride and dried over  $\text{MgSO}_4$ . The organic phase was evaporated *in vacuo* and purified by preparative layer chromatography, using hexane/ethyl acetate 40/60 (v/v) as eluent, affording (*S*)-**BPOH** as white powder (60 % yield).

**(S)-BPOHMe.** A solution of (*S*)-**BPOH** (59 mg, 0.23 mmol) and  $\text{SOCl}_2$  (2.4 mL) in MeOH (10 mL) was maintained under reflux for 2 h. The crude was rotavaporated, dissolved in methylene chloride and washed consecutively with saturated  $\text{NaHCO}_3$ , 1 M HCl and brine, then dried over  $\text{MgSO}_4$ . The solvent was evaporated *in vacuo*. Purification was done by preparative layer chromatography (hexane/ethyl acetate 70/30, v/v), affording (*S*)-**BPOHMe** as a white powder in nearly quantitative yield.

**Dyads (S,S)-1 and (S,R)-1.** To a solution of (*S*)-**BPOH** (56 mg, 0.23 mmol) in acetonitrile (20 mL), 0.23 mmol of EDC and 0.23 mmol of BtOH in acetonitrile were added. The mixture was maintained under stirring, and then 0.23 mmol of (*S*)- or (*R*)-**TrpMe** in 2 mL of acetonitrile were added. After 3 h, the solvent was evaporated; the crude was dissolved in methylene chloride and washed consecutively with diluted  $\text{NaHCO}_3$ , 1 M HCl and brine, then dried over  $\text{MgSO}_4$ . Final purification was performed by preparative layer chromatography (methylene chloride/ethyl acetate, 60/40, v/v), followed by recrystallization. The yields were 50 % and 47 % for (*S,S*)-**1** and (*S,R*)-**1**, respectively.

## Characterisation of the new compounds

All new compounds were characterised by  $^1\text{H}$  and  $^{13}\text{C}$  NMR spectroscopy, as well as by high resolution mass spectrometry (HRMS). Their purity was confirmed by gas chromatography (GC) and high performance liquid chromatography (HPLC). A summary of the most relevant data follows.

### Methyl (*S*)-2-(2-hydroxy-1,1'-biphenyl-4-yl)propanoate

$^1\text{H}$ -NMR ( $\text{CDCl}_3$ ) ( $\delta$ , ppm) 1.53 (d, 3H,  $J = 8.0$  Hz), 3.70 (s, 3H), 3.73 (q, 1H,  $J = 8.0$  Hz), 5.19 (s, 1H), 6.92-6.94 (m, 1H), 7.8-7.21 (m, 1H), 7.37-7.51 (m, 6H).  $^{13}\text{C}$ -NMR ( $\text{CDCl}_3$ ) ( $\delta$ , ppm) 18.5, 45.2, 52.1, 114.9, 119.4, 127.0, 127.9, 129.0, 129.3, 130.8, 136.8, 141.8, 152.5, 174.7. Exact Mass (ESI) [ $\text{MH}^+$ ] Calcd. for  $\text{C}_{16}\text{H}_{17}\text{O}_3$ : 257.1172; Found: 257.1181.

### *N*-[2-(*S*)-(2-Hydroxy-1,1'-biphenyl-4-yl)propanoyl]-(*R*)-tryptophan methyl ester.

$^1\text{H}$ -NMR ( $\text{CDCl}_3$ ) ( $\delta$ , ppm) 1.46 (d, 3H,  $J = 7.1$  Hz), 3.13-3.26 (m, 2H), 3.45 (q, 1H,  $J = 7.1$  Hz), 3.64 (s, 3H), 4.90 (m, 1H), 6.05 (d,

1H,  $J = 8.0$  Hz), 6.28 (s, 1H), 6.50 (d, 1H,  $J = 2.4$  Hz), 6.80 (m, 2H), 7.01-7.23 (m, 4H), 7.36-7.53 (m, 10H), 8.11 (bs, 1H).  $^{13}\text{C}$ -NMR ( $\text{CDCl}_3$ ) ( $\delta$ , ppm) 18.3, 27.5, 46.8, 52.6, 52.8, 109.5, 111.4, 115.1, 118.6, 119.7, 120.2, 122.2, 123.2, 127.5, 127.9, 129.0, 129.2, 130.9, 136.1, 137.5, 142.2, 153.3, 172.5, 173.9. Exact Mass (EI) [ $\text{M}^+$ ] Calcd. for  $\text{C}_{27}\text{H}_{26}\text{N}_2\text{O}_4$ : 442.1893; Found: 442.1897.

### ***N*-[2-(*S*)-(2-Hydroxy-1,1'-biphenyl-4-yl)propanoyl]-(*S*)-tryptophan methyl ester.**

$^1\text{H}$ -NMR ( $\text{CDCl}_3$ ) ( $\delta$ , ppm) 1.47 (d, 3H,  $J = 7.2$  Hz), 3.19-3.32 (m, 2H), 3.47 (q, 1H,  $J = 7.2$  Hz), 3.61 (s, 3H), 4.85 (m, 1H), 6.05 (d, 1H,  $J = 7.8$  Hz), 6.12 (s, 1H), 6.73-6.79 (m, 3H), 7.05-7.47 (m, 9H), 8.13 (bs, 1H).  $^{13}\text{C}$ -NMR ( $\text{CDCl}_3$ ) ( $\delta$ , ppm) 18.1, 27.4, 46.7, 52.4, 52.9, 109.9, 111.2, 115.1, 118.6, 119.7, 120.0, 122.2, 122.3, 127.2, 127.6, 127.7, 129.1, 130.7, 136.0, 137.1, 141.7, 152.9, 172.3, 173.3. Exact Mass (EI) [ $\text{M}^+$ ] Calcd. for  $\text{C}_{27}\text{H}_{26}\text{N}_2\text{O}_4$ : 442.1893; Found: 442.1891.

### **Fluorescence measurements**

Emission spectra were recorded on a spectrofluorometer system which was provided with a monochromator in the wavelength range of 200-900 nm. The solutions were placed into 10 mm  $\times$  10 mm quartz cells. The absorbance of the samples at the excitation wavelength was kept below 0.2. Steady state experiments were performed at 22 °C. For the fluorescence quantum yield determination, Trp in water/air was used as a reference, with  $\Phi_{\text{F}} = 0.13$ .<sup>17</sup>

Time-resolved fluorescence measurements were performed using the time-correlated single photon counting (TCSPC) technique. The excitation source was the third harmonic (267 nm) of a mode-locked Ti-Sapphire laser, delivering 100-fs pulses with a repetition rate of 4.75 MHz. A Schott WG 295 filter was placed in front of a SPEX monochromator. The detector was a microchannel plate (R1564 U Hamamatsu) providing an instrumental response function of 60 ps (fwhm). The average laser power (0.1 mW) was measured with a Melles Griot broadband powermeter. Solutions were contained in a 10 mm  $\times$  10 mm quartz cell and continuously stirred. Successive recordings with the same sample gave identical decays which were eventually merged to improve the signal-to-noise ratio. Such a procedure allowed us to ensure that the measured signals were not altered during the measurements due to a possible accumulation of photoproducts.

### **Acknowledgements**

Financial support from the Spanish Government (CTQ2010-14882, BES-2008-003314, JCI-2011-09926, PR2011-0581), from the Generalitat Valenciana (Prometeo 2008/090) and from the Universitat Politècnica de València (PAID 05-11, 2766) is gratefully acknowledged.

### **Notes and references**

<sup>50</sup> *a* Departamento de Química/Instituto de Tecnología Química UPV-CSIC, Universitat Politècnica de València, Camino de Vera s/n, 46022, Valencia, Spain. E-mail: [mcjimene@qim.upv.es](mailto:mcjimene@qim.upv.es); [mmiranda@qim.upv.es](mailto:mmiranda@qim.upv.es)

<sup>b</sup> CNRS, IRAMIS, SPAM, Francis Perrin Laboratory, URA 2453, 91191 Gif-sur-Yvette, France.

- 1 a) M. C. Jiménez, U. Pischel and M. A. Miranda, *J. Photochem. Photobiol. C*, 2007, **8**, 128-142; b) S. Abad, U. Pischel and M. A. Miranda, *J. Phys. Chem. A*, 2005, **109**, 2711-2717; c) S. Abad, I. Vayá, M. C. Jiménez, U. Pischel and M. A. Miranda, *ChemPhysChem*, 2006, **7**, 2175-2183.
- 2 a) P. Bonancía, I. Vayá, M. J. Climent, T. Gustavsson, D. Markovitsi, M. C. Jiménez and M. A. Miranda, *J. Phys. Chem. A*, 2012, **116**, 8807-8814; b) C. Paris, S. Encinas, N. Belmadoui, M. J. Climent and M. A. Miranda, *Org. Lett.*, 2008, **10**, 4409-4412; c) N. Belmadoui, S. Encinas, M. J. Climent, S. Gil and M. A. Miranda, *Chem. Eur. J.*, 2006, **12**, 553-561; d) V. Lhiaubet-Vallet, P. Boscá and M. A. Miranda, *J. Phys. Chem. B*, 2007, **111**, 423-431.
- 3 I. Vayá, R. Pérez-Ruiz, V. Lhiaubet-Vallet, M. C. Jiménez and M. A. Miranda, *Chem. Phys. Lett.*, 2010, **486**, 147-153.
- 4 J. R. Lakowicz, *Principles of Fluorescence Spectroscopy*, 3<sup>rd</sup> Edition; Plenum Press: New York, 2006.
- 5 a) N. Seedher and S. Bhatia, *J. Pharm. Biomed. Anal.*, 2005, **39**, 257-262; b) N. Seedher and S. Bhatia, *Pharmacol. Res.*, 2006, **54**, 77-84; c) R. K. Nanda, N. Sarkar and R. Banerjee, *J. Photochem. Photobiol. A*, 2007, **192**, 152-158; d) B. Zhou, R. Li, Y. Zhang and Y. Liu, *Photochem. Photobiol. Sci.*, 2008, **7**, 453-459; e) H. Vahedian-Movahed, M. R. Saberi and J. Chamani, *J. Biomol. Struct. Dyn.*, 2011, **28**, 483-502; f) U. Katrahalli, V. K. A. Kalabandi and S. Jaldappagari, *J. Pharm. Biomed. Anal.*, 2012, **59**, 102-108; g) M. El-Kemary, M. Gil and A. Douhal, *J. Med. Chem.*, 2007, **50**, 2896-2902; h) L. Tormo, J. A. Organero, B. Cohen, C. Martin, L. Santos and A. Douhal, *J. Phys. Chem. B*, 2008, **112**, 13641-13647; i) S. Tardioli, I. Lammers, J. H. Hooijschuur, F. Ariese, G. van der Zwan and C. Gooijer, *J. Phys. Chem. B*, 2012, **116**, 7033-7039.
- 6 I. Vayá, M. C. Jiménez and M. A. Miranda, *J. Phys. Chem. B*, 2007, **111**, 9363-9371.
- 7 a) P. R. Callis and B. K. Burgess, *J. Phys. Chem. B*, 1997, **101**, 9429-9432; b) J. R. Lakowicz, *Photochem. Photobiol.*, 2000, **72**, 421-437; c) B. Schuler and W. A. Eaton, *Curr. Opin. Struct. Biol.*, 2008, **18**, 16-26; d) X. H. Shen and J. R. Knutson, *J. Phys. Chem. B*, 2001, **105**, 6260-6265.
- 8 a) J. M. Beechem and L. Brand, *Annu. Rev. Biochem.*, 1985, **54**, 43-71; b) P. R. Callis, *Methods Enzymol.*, 1997, **278**, 113-150.
- 9 a) T. Peters, *All About Albumins: Biochemistry Genetics and Medical Applications*, Academic Press, San Diego, 1995; b) D. C. Carter, J. X. Ho, in *Advances in Protein Chemistry*, Vol. 45, Academic Press, New York, 1994, pp. 152-203.
- 10 a) N. Basaric and P. Wan, *J. Org. Chem.*, 2006, **71**, 2677-2686; b) M. Lukeman and P. Wan, *J. Am. Chem. Soc.*, 2003, **125**, 1164-1165.
- 11 a) J. Keck, H. E. A. Kramer, H. Port, T. Hirsch, P. Fischer and G. Rytz, *J. Phys. Chem.*, 1996, **100**, 14468-14475; b) F. Vollmer and W. Rettig, *J. Photochem. Photobiol. A*, 1996, **95**, 143-155.
- 12 M. Lukeman and P. Wan, *J. Am. Chem. Soc.*, 2002, **124**, 9458-9464.
- 13 M. C. Jiménez, M. A. Miranda, R. Tormos and I. Vayá, *Photochem. Photobiol. Sci.*, 2004, **3**, 1038-1041.
- 14 A. Weller, *Z. Phys. Chem.*, 1982, **133**, 93-98.
- 15 a)  $E_{\text{OX}}$  (2-phenylphenol) = 0.831 V, taken from: P. Winget, C. J. Cramer and D. G. Truhlar, *Theor. Chem. Acc.*, 2004, **112**, 217-227; b)  $E_{\text{RED}}$  (Trp) = -1.55 V, taken from: S. Cakir and E. Bicer, *J. Chil. Chem. Soc.*, 2010, **55**, 236-239; c)  $E_{\text{OX}}$  (indole) = 1.015 V,  $E_{\text{RED}}$  (biphenyl) = -2.55 V, taken from S. L. Murfov, I. Carmichael, and G. L. Hug, *Handbook of Photochemistry*, 2<sup>nd</sup> Edition; Marcel Dekker: New York, 1993. 8.
- 16 *Handbook of Chemistry and Physics*, 85<sup>th</sup> Edition; CRC Press: Boca Raton, FL, 2004.
- 17 M. Montalti, A. Credi, L. Prodi and M. T. Gandolfi, *Handbook of Photochemistry*, CRC Press, Taylor and Francis Group, Boca Raton FL, 2006.